

The 1.9 Å Resolution Structure of Phospho-serine 46 HPr from *Enterococcus faecalis*

Gerald F. Audette¹, Roswitha Engelmann³, Wolfgang Hengstenberg³
Josef Deutscher⁴, Koto Hayakawa¹, J. Wilson Quail² and
Louis T. J. Delbaere^{1*}

¹Department of Biochemistry
University of Saskatchewan
107 Wiggins Road, Saskatoon
Saskatchewan, S7N 5E5
Canada

²Department of Chemistry
University of Saskatchewan
110 Science Place, Saskatoon
Saskatchewan, S7N 5C9
Canada

³Department of Biology
University of Bochum
D-44780 Bochum, Germany

⁴Laboratoire de Genetique des
Microorganismes, INRA-
CNRS, F-78330, Thiverval-
Grignon, France

The histidine-containing phosphocarrier protein HPr is a central component of the phosphoenolpyruvate:sugar phosphotransferase system (PTS), which transfers metabolic carbohydrates across the cell membrane in many bacterial species. In Gram-positive bacteria, phosphorylation of HPr at conserved serine 46 (P-Ser-HPr) plays several regulatory roles within the cell; the major regulatory effect of P-Ser-HPr is its inability to act as a phosphocarrier substrate in the enzyme I reaction of the PTS. In order to investigate the structural nature of HPr regulation by phosphorylation at Ser46, the structure of the P-Ser-HPr from the Gram-positive bacterium *Enterococcus faecalis* has been determined. X-ray diffraction analysis of P-Ser-HPr crystals provided 10,043 unique reflections, with a 95.1% completeness of data to 1.9 Å resolution. The structure was solved using molecular replacement, with two P-Ser-HPr molecules present in the asymmetric unit. The final *R*-value and *R*_{Free} are 0.178 and 0.239, respectively. The overall tertiary structure of P-Ser-HPr is that of other HPr structures. However the active site in both P-Ser-HPr molecules was found to be in the “open” conformation. Ala16 of both molecules were observed to be in a state of torsional strain, similar to that seen in the structure of the native HPr from *E. faecalis*. Regulatory phosphorylation at Ser46 does not induce large structural changes to the HPr molecule. The B-helix was observed to be slightly lengthened as a result of Ser46 phosphorylation. Also, the water mediated Met51-His15 interaction is maintained, again similar to that of the native *E. faecalis* HPr. The major structural, and thus regulatory, effect of phosphorylation at Ser46 is disruption of the hydrophobic interactions between EI and HPr, in particular the electrostatic repulsion between the phosphoryl group on Ser46 and Glu84 of EI and the prevention of a potential interaction of Met48 with a hydrophobic pocket of EI.

© 2000 Academic Press

Keywords: histidine-containing phosphocarrier protein; PTS; P-Ser-HPr; phosphorylation; X-ray crystallography

*Corresponding author

Abbreviations used: PTS, phosphoenolpyruvate:sugar phosphotransferase system; HPr, histidine-containing phosphocarrier protein of the PTS; P-Ser-HPr, phospho-serine 46 HPr; P-His-HPr, phospho-histidine 15 HPr; EI, enzyme I of the PTS; NCS, non-crystallographic symmetry; CcpA, catabolite control protein A; GK, glycerol kinase.

E-mail address of the corresponding author:
louis.delbaere@usask.ca

Introduction

The histidine-containing phosphocarrier protein HPr is part of the phosphoenolpyruvate-dependent bacterial phosphotransferase system (PTS), which plays a central role in bacterial metabolism. The PTS is primarily responsible for the detection, migration towards, and concurrent phosphorylation and uptake of metabolic carbohydrates.^{1,2} The PTS catalyzes the transfer of an activated phosphoryl group from phosphoenolpyruvate (PEP) to the imported sugar upon transfer across

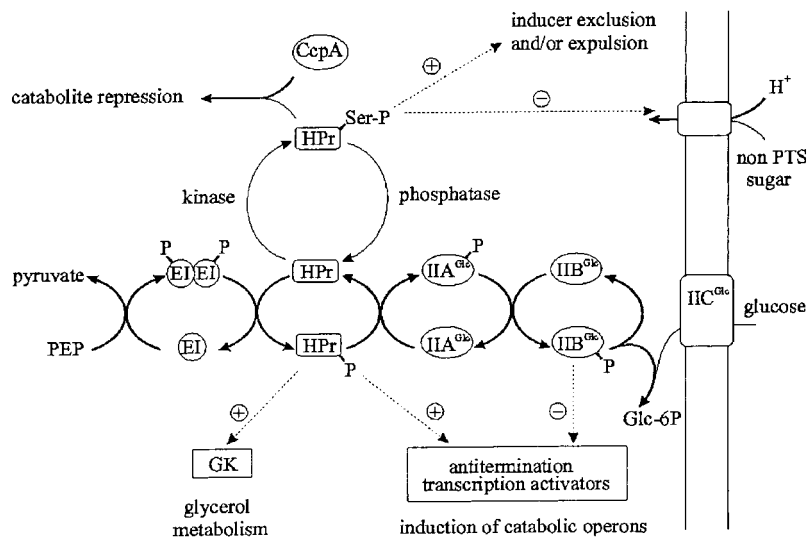


Figure 1. The role of HPr in bacterial carbohydrate metabolism. In the presence of small amounts of glucose or other PTS sugars, cellular levels of ATP are low, resulting in HPr being unphosphorylated at Ser46. This allows HPr to transfer a phosphoryl group from PEP through EI down the PTS to the sugar as it is being imported into the cell. In the presence of large concentrations of carbohydrate, cellular ATP levels are increased, resulting in the phosphorylation of HPr at Ser46. This results in PTS down-regulation due to P-Ser-HPr's inability to accept a phosphoryl group from EI. P-Ser-HPr is also able to inhibit non-PTS carbohydrate uptake directly through inducer exclusion

and/or expulsion,^{40,41} as well as influence metabolic gene expression through interaction with CcpA. Abbreviations: CcpA, catabolite control protein A; GK, glycerol kinase.

the bacterial cell membrane (Figure 1). Proteins of the PTS are also involved in regulation of carbohydrate uptake at the level of gene expression or directly influence the catalytic activities of enzymes. A well-studied example of this regulation is the glucose-specific Enzyme IIA (EIIA^{Glc}) of the PTS in *Escherichia coli* (reviewed in 3,4). In its phosphoform, EIIA^{Glc} activates adenylate cyclase which produces cAMP as a ligand for the catabolite gene activator protein known to enhance transcription of catabolic genes in the absence of glucose. In the dephosphorylated state, which occurs in the presence of glucose, EIIA^{Glc} inhibits the influx of lactose into the bacterium and thus prevents induction of the lac operon. This scenario is well known as catabolite repression in Gram-negative bacteria.

In Gram-positive bacteria, a different mechanism of catabolite repression operates by which HPr is phosphorylated at Ser46 by the ATP-dependent HPr kinase/phosphatase.⁵⁻⁸ The resulting phospho-serine HPr is only slowly phosphorylated at His15 by the PEP-dependent enzyme I (EI). The kinase activity of the bifunctional HPr-kinase/phosphatase is stimulated by high ATP levels in glycolysing bacteria. In starving bacteria the P-Ser-HPr phosphatase activity is dominant.⁸ As a result, PEP-dependent uptake and phosphorylation of metabolic carbohydrates is strongly inhibited in the presence of glucose.⁹ Beside this direct regulation of the HPr activity, P-Ser-HPr forms a complex with the catabolite control protein A (CcpA) which binds to the operator-like catabolite responsive element (CRE) sequence. CRE elements are common motifs in front of many operons involved in carbohydrate degradation. Thus, P-Ser-HPr is also involved in the regulation of gene expression.^{10,11}

Regulatory phosphorylation by phosphotransfer from the imidazole ring of His15 of HPr is known to occur during antitermination. The antiterminator proteins of the *bgl-sac* family are regulated by phosphorylation at conserved histidine residues in the PTS regulatory domains (PRDs). Transcription of several operons involved in carbohydrate utilization appears to be controlled by this mechanism.¹² Recently HPr was shown to allosterically stimulate glycogen phosphorylase in *Escherichia coli*.¹³ It has been shown that in Gram-positive bacteria, glycerol kinase is activated by PEP-dependent phosphorylation at a single histidine residue by P-His-HPr.¹⁴

In recent years genes of numerous carbohydrate-specific PTS proteins, as well as the genes of the general specificity PTS proteins EI and HPr, have been cloned and can be easily overexpressed in large amounts as recombinant proteins. This has greatly stimulated research into the elucidation of the three-dimensional structures of PTS proteins. The structures of HPr from several bacterial species have been solved using X-ray diffraction and high-resolution multidimensional NMR methods (reviewed in 15). Recently, the structure of the N-terminal domain of enzyme I (EIN) in complex with HPr of *E. coli* was determined by NMR.¹⁶

In this context, the structure of P-Ser-HPr, known to be a poor substrate of EI, is essential. It has been proposed^{17,18} that the regulatory nature of phosphorylation of HPr at conserved Ser46 in Gram-positive bacteria could be due to any one or all of the following: (a) movement or conformational change of the B-helix (residues Ser46 to Leu53); (b) alteration of the Met51-His15 interaction, resulting in an inaccessibility or alteration of the electrostatic potential of the active center microenvironment; and (c) alteration of the microenvi-

onment required for PTS protein interaction, in particular interaction with EI. In order to address this question, we have determined the crystal structure of P-Ser-HPr from the Gram-positive bacteria *Enterococcus faecalis* to 1.9 Å resolution.

Results and Discussion

The final model consists of two molecules of P-Ser-HPr within the asymmetric unit, related by non-crystallographic symmetry (NCS). The structure was refined to 1.9 Å resolution (diffraction data summarized in Table 1). The final model consists of 87 amino acid residues per P-Ser-HPr molecule, numbered 1-87 and 101-187 for the first and second molecule respectively, and 91 solvent (water) molecules. The stereochemical quality of the final model was analyzed using the program PROCHECK.¹⁹ A total of 94.7% of the amino acid residues are within the most favored regions of the Ramachandran plot.²⁰ The remaining residues (5.3%) are located within additional allowed regions, notably Ala16 and Ala116, which are observed to be in a region of torsional strain. The mean coordinate error from Luzatti plot analysis²¹ is 0.1 Å, and the r.m.s. deviation between the α -carbon atoms of molecules I and II is 0.27 Å. The final refinement statistics are summarized in Table 2.

The overall architecture of the HPr molecule has been described as an open faced β -sandwich, with a $\beta\alpha\beta\beta\alpha\beta\alpha$ secondary structural arrangement. This architecture is highly conserved among all HPr structures studied to date.¹⁵ As expected, due to the knowledge that the ATP-dependent HPr kinase/phosphatase is a bifunctional enzyme with a single active site,⁸ phosphorylation of Ser46 does not impart a large conformational change to the overall folding of the HPr molecule (Figure 2). A comparison between HPr molecules indicates only slight differences; the average r.m.s. differences between the α -carbon atoms of both molecules of P-Ser-HPr and the native *E. faecalis* HPr,¹⁷ native *Bacillus subtilis* HPr,²² Ser46Asp mutant HPr from *B. subtilis*²³ and the Ser46Asp mutant HPr from *E. coli*¹⁸ are 0.41 Å, 0.75 Å, 0.71 Å, and 1.27 Å, respectively.

Serine 46 caps the B-helix, an eight-residue α -helix consisting of residues Ser46 to Leu53. It

Table 1. Data collection statistics for P-Ser-HPr

Diffraction data	All data	Last shell
Resolution range	40-1.90 Å	1.93-1.90 Å
No. reflections measured	42,471	1668
No. of unique reflections	10,043	447
Completeness (%)	95.1	84.3
R_{Symm} ^a	0.04	0.11
Mean $I/\sigma(I)$	8.6	5.3

^a $R_{\text{Symm}} = \sum_j |I_j - \langle I \rangle| / \sum_j I_j$ where j = a set of observations of equivalent reflections and $\langle I \rangle$ = average intensity of the reflection.

Table 2. Summary of refinement statistics

A. Diffraction agreement	
Resolution range (Å)	40-1.90
R-value ^{a,b}	0.178
R_{Free} ^c	0.239
No. of unique reflections	10,043
B. Quality of structure	
Model parameters	
Total protein non-H atoms	1292
Solvent molecules	91
B-factor model	Individual Isotropic
Mean B-factors (Å ²)	
Molecule I - Main-chain	11.7
- Side-chain	18.5
- Phosphoryl group	25.9
Molecule II - Main-chain	10.0
- Side-chain	16.1
- Phosphoryl group	31.3
Water molecules	28.0
C. r.m.s.d from stereochemical ideality	
Bonds (Å)	0.01
Angles (deg.)	1.59
Dihedrals (deg.)	22.93
Impropers (deg.)	1.15

^a R-value = $\sum_{hkl} |F_o - F_c| / \sum_{hkl} |F_o|$.

^b All data, final refinement cycle.

^c Randomly chosen test set of 5% of unique reflections (496 reflections).

has been postulated that phosphorylation of Ser46 would result in movement or conformational change in the B-helix, which would communicate to the active site.¹⁷ Napper and coworkers¹⁸ study of the Ser46Asp mutant of the *E. coli* HPr indicated that the B-helix became more compressed in comparison to the native *E. coli* HPr. The compression of the B-helix due to the Ser46Asp mutation was modest, with an average decrease in N—O hydrogen bond distances being 0.15 Å. Thus, it was felt that these conformational changes in the B-helix might result in the inability of Ser46Asp HPr, and by extrapolation P-Ser-HPr, to accept the phosphoryl group from EIN at His15.

Phosphorylation of Ser46 does not induce a large conformational change on the B-helix (Figure 3), and only slight differences in the overall polypeptide chain folding between HPr molecules are noted. Also, the α -helical nature of the B-helix is retained throughout the small B-helix in both P-Ser-HPr molecules. This is unlike the Ser46Asp HPr mutant from *E. coli*¹⁸ in which the B-helix shifted from an α to a 3_{10} helix at residue 48. Lastly, the N—O hydrogen bond distances are seen to lengthen by an average of 0.13 Å from the native *E. faecalis* HPr (Table 3). Thus the regulatory nature of phosphorylation of Ser46 in Gram-positive bacteria is likely not due to an induced compression of nor a conformational change in the B-helix.

The interaction between Met51 and His15 of the active site has also been proposed to be a means of HPr inactivation by phosphorylation at Ser46.¹⁷ The carbonyl oxygen atom of Met51 was seen to interact with NE2 of His15 *via* a bridging water

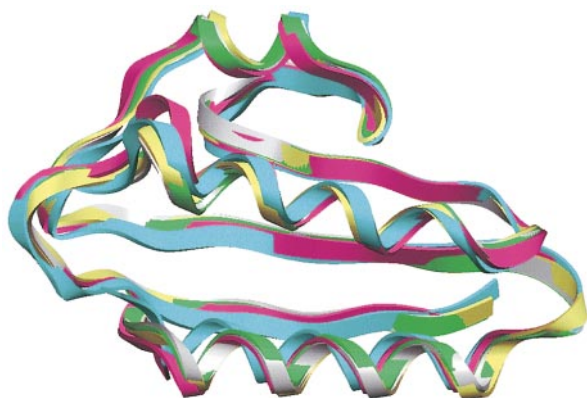


Figure 2. Ribbon representation of the superposition of the C α trace of four different HPr structures. Molecules I and II of P-Ser-HPr are shown in yellow and magenta, respectively, the native HPr from *E. faecalis*¹⁷ in cyan, native HPr from *B. subtilis*²³ in gray, and the Ser46Asp mutant HPr from *E. coli* (a P-Ser-HPr analog)¹⁸ in teal. Figures 2 to 5 were produced using the program SETOR.⁴²

molecule. His15 was also observed to interact with Thr12 *via* a direct hydrogen bond from ND1 to the main-chain carbonyl oxygen atom of Thr12. It was proposed that upon phosphorylation, a conformational change in the B-helix might result in either a direct blockage of the active site by the B-helix or an indirect effect through alteration of the

Met51(CO)-His15(NE2) water-bridged interaction. With the above noted lengthening of the B-helix, it can be inferred that there is not a direct blockage of the active site by the B-helix. Also, modest differences in the Met51 to His15 distances are seen to occur upon phosphorylation (Table 4, Figure 4), with an average decrease of 0.44 Å in the Met51-His15 distance; this decrease in Met51(CO)-His15(NE2) distance is compensated by the bridging water molecule. For P-Ser-HPr molecule I, the Met51(CO)-Wat distance decreases by 0.22 Å, and the Wat-His15(NE2) distance decreases by 0.26 Å from that seen in the native HPr from *E. faecalis*. The active-site histidine residue of molecule I is also held in position by a hydrogen bond from ND1 to the main-chain carbonyl oxygen atom of Thr12, similar to that of the native HPr from *E. faecalis*.

The active-site histidine residue of P-Ser-HPr molecule II differs from both molecule I and the native *E. faecalis* HPr. The side-chain of His115 was observed to be rotated about the C α -C β bond (Figure 4). As a result of this rotation, ND1 of His115 is in contact with the main-chain carbonyl oxygen atom of Met51 through the bridging water molecule. This is unlike P-Ser-HPr molecule I and the native *E. faecalis* HPr, in which His15 interacts with Met51 *via* NE2 through the bridging water molecule. There was however, no decrease in Met51(CO)-Wat distance, and only a slight (0.25 Å) decrease in the Wat-His15(ND1) distance. The NE2 of His115 is stabilized by hydrogen bonding

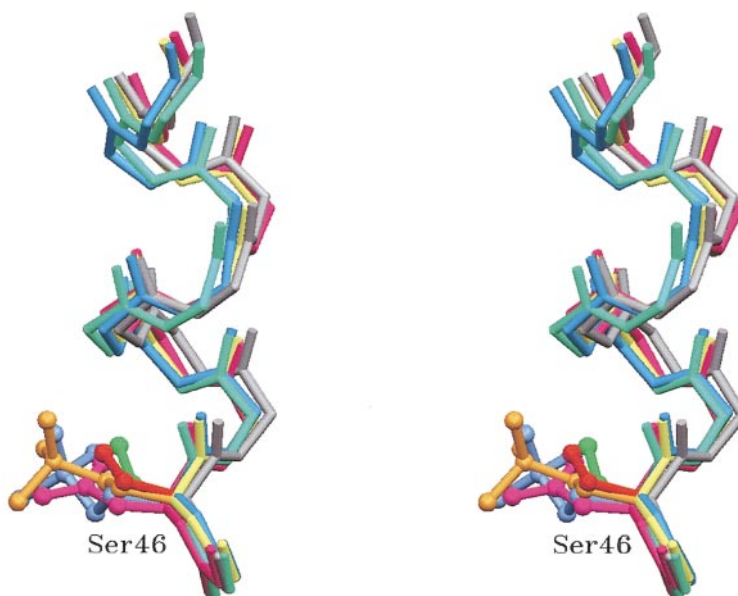


Figure 3. Superposition of the main-chain atoms in the helix-B region of both P-Ser-HPr molecules, native HPrs from *E. faecalis* and *B. subtilis* and the Ser46Asp mutant HPr from *E. coli*. There are no major differences between HPr molecules observed in this region, and the average r.m.s. difference between α -carbon atoms is 0.81 Å between these HPr molecules. Therefore, regulatory phosphorylation does not induce a large conformational effect upon the B-helix. Colors (main-chain and side-chain) are yellow and gold for P-Ser-HPr molecule I, magenta and light blue for molecule II of P-Ser-HPr, cyan and red for the native *E. faecalis* HPr,¹⁷ gray and green for the native *B. subtilis* HPr²³ and teal and purple for the Ser46Asp mutant HPr of *E. coli*.¹⁸

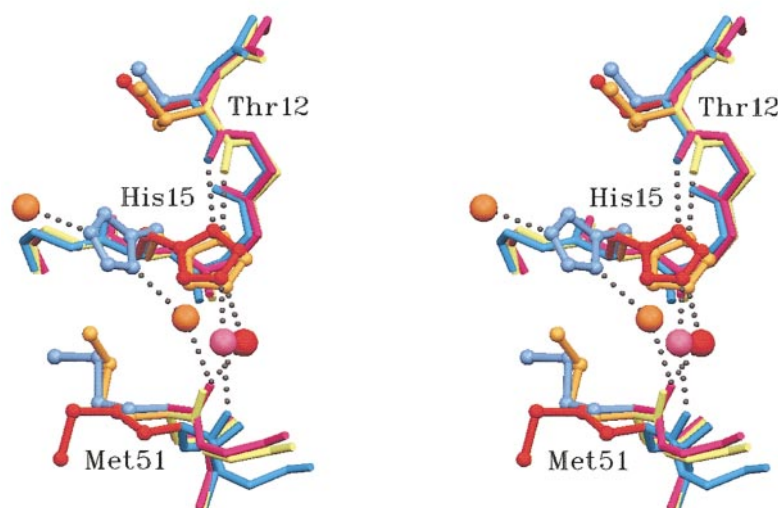


Figure 4. Signaling to the active site? The interaction between Met51(CO) and His15 of the active site was proposed to be a means of HPr inactivation by phosphorylation at Ser46.¹⁷ Shown is a superposition of the main-chain atoms of both molecules of P-Ser-HPr and the native *E. faecalis* HPr. Colors (main-chain and side-chain) are yellow and gold for P-Ser-HPr molecule I, magenta and light blue for molecule II of P-Ser-HPr, cyan and red for the native *E. faecalis* HPr, with Wat139 of the native *E. faecalis* HPr in pink, Wat255 of P-Ser-HPr molecule I in red, and Wat253 and 288 of P-Ser-HPr molecule II in orange. Interatomic distances between Met51 and His15 are indicated in Table 4.

through Water288 to a network of ordered water molecules, rather than to Thr12. Noting that there is an average r.m.s.d. of 0.41 Å between the P-Ser-HPr molecules and that of the native *E. faecalis* HPr, the modest differences in side-chain-to-water molecule distances are not believed to result in a signaling from the B-helix to the active site upon Ser46 phosphorylation. It is also likely that the differences in His15 orientation between P-Ser-HPr molecules I and II are due to the inherent flexibility of the active site and is not a result of Ser46 phosphorylation.

The active site of HPr is comprised of residues His15 and Arg17, which are conserved among all HPrs. These two active-site residues are fully surface exposed at the N terminus of the A-helix, and are separated by a single non-conserved amino acid residue. X-ray diffraction analysis of the native HPr from *E. faecalis* indicated that the active site was in an “open” conformation.^{17,24} In this conformation, His15 and Arg17 were observed to be pointing away from one another with a distance between NE2 of His15 and NH2 of Arg17 of ~18 Å, the maximum possible distance. The “closed” conformation of the HPr active site exhibits smaller distances between His15-NE2 and Arg17-NH2; for example 11.1 Å for the Ser46Asp mutant from *E. coli*,¹⁸ 6.7 Å for the native HPr from *B. subtilis*,²² and 8.0 Å for the Ser46Asp

mutant of *B. subtilis*.²³ Also, Ala16 was observed to be in a state of torsion angle strain ($\phi = 59^\circ$, $\psi = -153^\circ$). Previously, the native *E. faecalis* HPr was the only HPr structure which exhibits this strain.

In the present X-ray analysis, both molecules of P-Ser-HPr are seen to be in the open conformation; the average distance between NE2 of His15 and NH1/NH2 of Arg17 is 16.7 Å and 15.2 Å for P-Ser-HPr molecule I and II, respectively. Also, both Ala16 and Ala116 exhibit a similar torsionally strained conformation, with ϕ , ψ angles of 57° , -144° and 63° , -154° for Ala16 and Ala116, respectively. While it is possible that this torsion angle strain seen at Ala16 is due to crystal packing,¹⁵ the present analysis does not lend to this conclusion. Ala16 makes only one contact with a symmetry-related molecule, this being a very weak interaction between the CO of Ala16 and NE2 of His7 (3.57 Å). Similarly, the CO of Ala116 interacts with the NE2 of a symmetry related His7 (3.93 Å). These intermolecular contacts observed between the P-Ser-HPr molecules and symmetry-related molecules are weak, whereas several stronger interactions would likely be observed in this region to indicate crystal packing forces dictating the conformation of Ala16. Also, as noted above it was observed that the side-chain of His15 adopts a different orientation between molecules I and II,

Table 3. Comparison of the hydrogen bond distances seen in helix-B of native HPr from *E. faecalis* and P-Ser-HPr

Donor	Acceptor	Hydrogen bond (N—O) distance (Å)		Change from native (Å)
		P-Ser-HPr ^a	Native <i>E. faecalis</i> HPr	
V50-N	S46-O	3.22	2.96	+0.26
M51-N	I47-O	2.96	2.86	+0.10
S52-N	M48-O	2.98	2.91	+0.07
L53-N	G49-O	3.26	3.17	+0.09

^a The P-Ser-HPr distances are an average of the distances observed in the two individual P-Ser-HPr molecules.

Table 4. Met51-His15 interactions and the role of water

HPr Molecule	M51 ^a -H15 ^b distance (Å)	Change from native (Å)	Bridging water molecule	M51-W (Å)	W-H15 (Å)
P-Ser-HPr I	3.96 (NE2)	-1.03	W255	2.52	2.72
P-Ser-HPr II	5.15 (ND1)	+0.16	W253	2.76	2.73
Native <i>E. faecalis</i>	4.99 (NE2)	-	W139	2.77	2.98

^a Met51 interacts with His15 through its main-chain carbonyl oxygen atom.

^b The His15 atom which interacts with the Met51 CO *via* the bridging water is noted in parenthesis.

due to a rotation about the C^α-C^β bond (Figure 4) and yet the torsion angle strains are similar in both molecules.

Regulatory phosphorylation at Ser46 does not appear to induce large structural changes to HPr, in particular in the region of the active site. Thus, it is believed that the effect of phosphorylation is to inhibit interaction with EI, and thus prevent PTS phosphoryl group transfer and make HPr available for catabolite repression in the presence of glucose (Figure 1). The recent analysis of the EIN:HPr complex from *E. coli* using NMR spectroscopy¹⁶ indicated that the site of interaction between EIN and HPr is mainly hydrophobic, although some electrostatic and hydrogen bonding interactions were observed. In particular, Ser46 of HPr was seen to be involved in a hydrogen bond with Glu84 of EIN. Therefore, a consequence of HPr phosphorylation at Ser46 would be that this latter interaction would be disrupted due to a repulsion of the negative charges and that proper interaction between EIN and HPr would not be possible to allow for phosphotransfer.

In order to examine the role of Ser46 phosphorylation on EI:HPr interaction, both molecules of P-Ser-HPr and the native *E. faecalis* HPr were superimposed onto the HPr of the EIN:HPr complex¹⁶ (Figure 5). In the *E. coli* complex, Phe48 of HPr makes hydrophobic interactions with six residues of EIN (Leu79, Asp82, Leu85, Ile108, Gln111, and Val130) which form a hydrophobic pocket in which Phe48 sits. Examination of the native HPr from *E. faecalis* indicates that Met48 occupies a similar region (Figure 5(a)), and thus is likely to make similar van der Waals contacts with EI. Also, Ser46 of the native *E. faecalis* HPr would be able to hydrogen bond to Glu84 of EI, as is seen in the NMR complex. Examination of both molecules of P-Ser-HPr superimposed onto the HPr of the NMR complex (Figure 5(b)), indicate that the electrostatic repulsion between the Glu84 side-chain by the phosphoryl group on Ser46 may be reduced with rotation about the Ser46 C^α-C^β bond. This rotation would position the phosphoryl group close to the hydrophobic pocket in which Met48 would sit in order to hydrogen bond with Glu84 of EI. This would force Met48 out of the pocket and result in a disruption of the hydrophobic interaction between HPr and EI, preventing PTS phosphoryl group transfer. It is also possible that due to the electrostatic repulsion between the Glu84 side-

chain of EI and the P-Ser46 of HPr, the HPr molecule could not fully approach EI, again preventing PTS phosphoryl group transfer by prevention of the required hydrophobic interactions. This prevention of EI:HPr interaction would free P-Ser-HPr from the PTS and make it available for catabolite repression through interaction with CcpA in the presence of large amounts of glucose.

Materials and Methods

Phospho-serine 46 HPr (P-Ser-HPr) from *E. faecalis* was purified as described.²⁵ Crystals were grown using the hanging-drop vapor diffusion method. Drops of 4 μl containing 5 mg/ml protein and 1.4 M sodium-potassium phosphate (pH 4.2) were equilibrated over a 1 ml reservoir containing 2.8 M sodium-potassium phosphate (pH 4.2). Diffraction-quality crystals were grown by seeding drops with smaller washed crystals using the method by Thaller *et al.*²⁶ Crystals are clear rods of average dimensions 0.3 mm × 0.15 mm × 0.15 mm, which crystallize in the monoclinic space group *P*2₁, with unit cell dimensions *a* = 25.52 Å, *b* = 43.20 Å, *c* = 60.75 Å, and β = 92.67°. Two molecules of P-Ser-HPr are present within the asymmetric unit, with a Matthews coefficient²⁷ of 1.9 Å³/Da and an estimated 31.3% (v/v) solvent content.

High-resolution diffraction data were collected at beamline BL18B of the Photon Factory synchrotron radiation facility in Tsukuba, Japan. Diffraction data were collected from a single crystal at 290 K on a Fuji BASIII imaging plate (400 mm × 800 mm) with the screenless Weissenberg camera (radius 429.7 mm),²⁸ using 13 images of 15° oscillations and 0.5° overlap per image. The data were digitized using a Rigaku drum scanning system, and processed using the DENZO/SCALEPACK software package.²⁹ A total of 42,471 reflections were collected to a resolution of 1.9 Å, with an average crystal mosaicity of 0.253°. These 42,471 reflections were merged to yield 10,043 unique reflections (*R*_{Symm} = 0.041), and the data is 95.1% complete to 1.9 Å. A summary of data collection statistics is shown in Table 1.

The molecular replacement method was used to solve the structure of P-Ser-HPr using the program AMoRe of the CCP4 software package.^{30,31} The initial search model was the native HPr from *E. faecalis* (PDB accession code 1PTF).¹⁷ In order to determine the initial positions of the two molecules within the asymmetric unit, the top three peaks from the initial rotation search were used in the translation search. The top peak from this search was then referred to as molecule I. With molecule I fixed, the position of the second molecule was determined with respect to molecule I. After obtaining the initial coordinates for both molecules, rigid-body refinement in

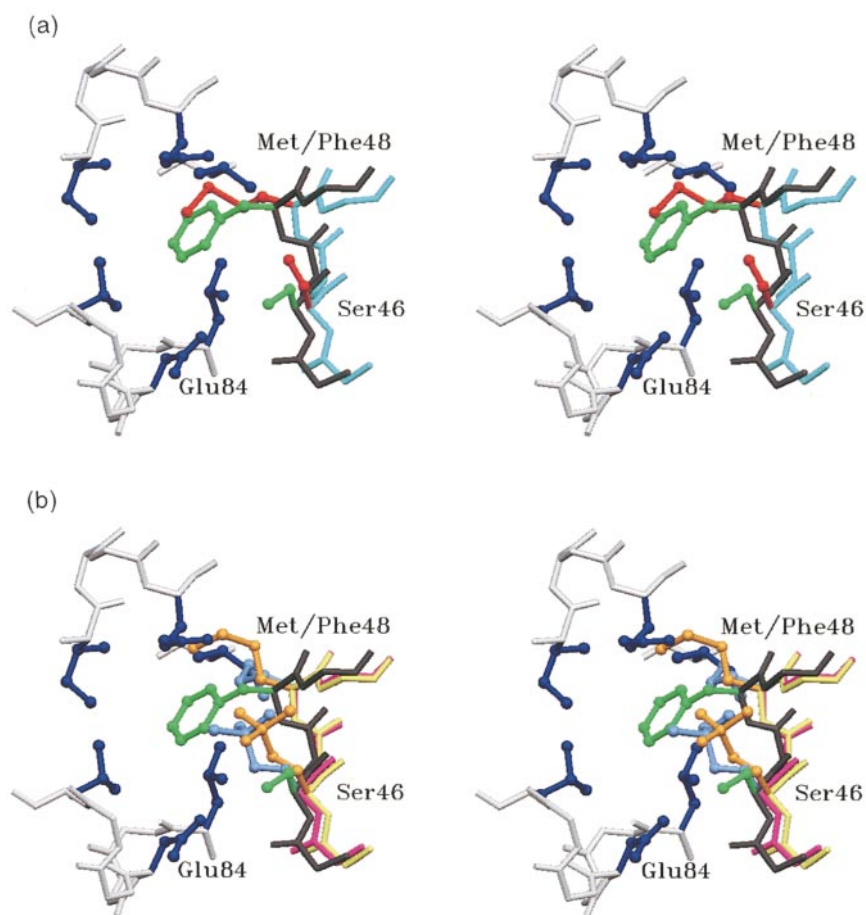


Figure 5. Regulation of EI:HPr interaction by Ser46 phosphorylation. (a) The native HPr from *E. faecalis* superimposed upon that of the HPr of the EIN complex indicates that Ser46 of both molecules hydrogen bonds with Glu84 of EI. Also, Met48 of the *E. faecalis* HPr occupies a similar position as Phe48 of the *E. coli* enzyme. This would allow for hydrophobic interactions in the unphosphorylated state. (b) Both P-Ser-HPr molecules are superimposed upon that of the HPr from the complex. It can be seen that in order for the phosphoryl group at Ser46 to interact with Glu84 of EI, the phosphoryl group is rotated into the hydrophobic pocket in which Met48 would sit. This would disrupt the hydrophobic interactions between HPr and EI, thus preventing PTS phosphoryl transfer. Colors (main-chain and side-chain) are yellow and gold for P-Ser-HPr molecule I, magenta and light blue for molecule II of P-Ser-HPr, cyan and red for the native *E. faecalis* HPr,¹⁷ and Enzyme I and HPr of the Garrett *et al.*¹⁶ are in gray and blue and dark gray and green (main-chain and side-chain), respectively.

AMoRe resulted in a correlation coefficient and R -value of 0.726 and 0.357, respectively.

Upon examination of the initial electron density map, using the TURBO-FRODO software package,³² density in a $|2F_o - F_c|$ map was observed to correspond to a phosphoryl group at Ser46 of both molecules. This group was added to the side-chain of Ser46 of both molecules using modified sulfate coordinates obtained from the Hetero-compound Information Center in Uppsala (HIC-Up), Sweden.³³ Rounds of model building were followed by simulated annealing refinement, B -factor refinement and new SIGMAA weighted^{34,35} electron density map generation using X-PLOR.^{36,37} The two P-Ser-HPr molecules within the asymmetric unit are related by non-crystallographic symmetry (NCS) rotation and translation operations.

Of the 10,043 unique reflections, 5% of the reflections were randomly chosen to evaluate R_{Free} .³⁸ All cycles of structure refinement, with exception of the final cycle, used a working set consisting of 95% of the unique reflections and a test set consisting of the 5% randomly

chosen reflections. The final cycle of refinement used all data. The simulated annealing refinements consisted of a prestage of 160 cycles of minimization followed by a slow-cooling stage starting at 3000 K in steps of 50 K and a timestep of 0.5 fs. Slow-cooling was followed by 120 cycles of conjugate gradient minimization and 40 cycles of B -factor refinement. Engh & Huber³⁹ bond and angle parameters were employed throughout refinement, and weighting was obtained from the CHECK procedure in X-PLOR. During initial cycles of refinement, NCS restraints were applied to the main-chain atoms only, but NCS restraints were removed for the final cycles of refinement. Water molecules were placed into the structure manually using a difference map. Upon refinement, some water molecules developed large B -factors ($>40 \text{ \AA}^2$). These were removed from the structure and new water molecules added as they were located in subsequent difference maps. The final R -value and R_{Free} of the structure are 0.178 and 0.239 respectively, and the final refinement statistics are summarized in Table 2. Examination of the differences between HPr molecules

was performed using the program LSQKAB of the CCP4 suite³⁰ by superposing the α -carbon atoms of the HPr molecules. The coordinates and structure amplitudes have been deposited in the Protein Data Bank (accession code 1FU0).

Acknowledgements

We gratefully acknowledge Drs L. Prasad and S. Napper for their helpful discussions. We thank Drs M. Suzuki, N. Watanabe and N. Sakabe (Photon Factory) for assistance during data collection. G.F.A. gratefully acknowledges financial support from the Colleges of Graduate Studies and Medicine from the University of Saskatchewan. This work was supported by a Medical Research Council of Canada operating grant to LTJD (MT-10162) and a Natural Sciences and Engineering Research Council of Canada operating grant to JWQ.

References

- Meadow, N. D., Fox, D. K. & Roseman, S. (1990). The bacterial phosphoenolpyruvate: glycolate phosphotransferase system. *Annu. Rev. Biochem.* **59**, 497-542.
- Postma, P. W., Lengeler, J. W. & Jacobson, G. R. (1993). Phosphoenolpyruvate: carbohydrate phosphotransferase systems of bacteria. *Microbiol. Rev.* **57**, 543-594.
- Lengeler, J. W., Jahreis, K. & Wehmeier, U. F. (1994a). Enzymes II of the phosphoenolpyruvate-dependent phosphotransferase systems: their structure and function in carbohydrate transport. *Biochim. Biophys. Acta.* **1188**, 1-28.
- Lengeler, J. W., Jahreis, K. & Lux, R. (1994b). Signal transduction through phosphotransferase system. In *Phosphate in Microorganisms: Cellular Biology* (Torriani-Gorini, A., Yagil, E. & Silver, S., eds), pp. 182-188, American Society for Microbiology, Washington, DC.
- Galinier, A., Kravanja, M., Engelmann, R., Hengstenberg, W., Kilhoffer, M.-C., Deutscher, J. & Haiech, J. (1998). New protein kinase and protein phosphatase families mediate signal transduction in bacterial catabolite repression. *Proc. Natl Acad. Sci. USA*, **95**, 1823-1828.
- Reizer, J., Hoischen, C., Titgemeyer, F., Rivolta, C., Rabus, R., Stülke, J., Karamata, D., Saier, M. H. & Hillen, W. (1998). A novel protein kinase that controls carbon catabolite repression in bacteria. *Mol. Microbiol.* **27**, 1157-1169.
- Brochue, D. & Vadeboncoeur, C. (1999). The HPr(Ser) kinase of *Streptococcus salivarius*: purification, properties and cloning of the *hprK* gene. *J. Bact.* **181**, 709-717.
- Kravanja, M., Engelmann, R., Dossonnet, V., Blüggel, M., Meyer, H. E., Frank, R., Galinier, A., Deutscher, J., Schnell, N. & Hengstenberg, W. (1999). The *hprK* gene of *Enterococcus faecalis* encodes a novel bifunctional enzyme: the HPr kinase/phosphatase. *Mol. Microbiol.* **31**, 59-66.
- Deutscher, J., Kessler, U., Alpert, C. A. & Hengstenberg, W. (1984). Bacterial phosphoenolpyruvate:sugar phosphotransferase system: P-Ser-HPr and its possible regulatory function. *Biochemistry*, **23**, 4455-4460.
- Deutscher, J., Küster, E., Bergstedt, U., Charrier, V. & Hillen, W. (1995). Protein kinase-dependent HPr/CcpA interaction links glycolytic activity to carbon metabolism in Gram-positive bacteria. *Mol. Microbiol.* **15**, 1049-1053.
- Jones, B. E., Dossonnet, V., Kuester, E., Hillen, W., Deutscher, J. & Klevit, R. E. (1997). Binding of catabolite repressor protein CcpA to its DNA target is regulated by phosphorylation of its corepressor HPr. *J. Biol. Chem.* **272**, 26530-26535.
- Stülke, J., Arnaud, M., Rapoport, G. & Martin-Verstraete, I. (1998). PRD - a protein domain involved in PTS-dependent induction and carbon catabolite repression of catabolic operons in bacteria. *Mol. Microbiol.* **28**, 865-874.
- Seok, Y.-J., Sondej, M., Badawi, P., Lewis, M. S., Briggs, M. C., Jaffe, H. & Peterkofsky, A. (1997). High-affinity binding and allosteric regulation of *Escherichia coli* glycogen phosphorylase by the histidine containing phosphocarrier protein HPr. *J. Biol. Chem.* **272**, 26511-26521.
- Charrier, V., Buckley, A., Parsonage, D., Galinier, A., Darbon, E., Jaquinod, M., Forest, E., Deutscher, J. & Claiborne, A. (1997). Cloning and sequencing of two enterococcal *glpK* genes and regulation of the encoded glycerol kinases by phosphoenolpyruvate-dependent phosphotransferase system-catalyzed phosphorylation of a single histidyl residue. *J. Biol. Chem.* **272**, 14166-14174.
- Waygood, E. B. (1998). The structure and function of HPr. *Biochem. Cell Biol.* **76**, 359-367.
- Garrett, D. S., Seol, Y.-J., Peterkofsky, A., Gronenborn, A. M. & Clore, G. M. (1999). Solution structure of the 40,000 M_r phosphoryl transfer complex between the N-terminal domain of enzyme I and HPr. *Nature Struct. Biol.* **6**, 166-173.
- Jia, Z., Vandonselaar, M., Hengstenberg, W., Quail, J. W. & Delbaere, L. T. J. (1994). The 1.6 Å structure of histidine-containing phosphotransfer protein HPr form *Enterococcus faecalis*. *J. Mol. Biol.* **236**, 1341-1355.
- Napper, S., Anderson, J. W., Georges, F., Quail, J. W., Delbaere, L. T. J. & Waygood, E. B. (1996). Mutation of serine-46 to aspartate in the histidine-containing protein of *Escherichia coli* mimics the inactivation by phosphorylation of serine-46 in HPrs from gram-positive bacteria. *Biochemistry*, **35**, 11260-11267.
- Laskowski, R. A., MacArthur, M. W., Moss, D. S. & Thornton, J. M. (1993). PROCHECK: a program to check the stereo chemical quality of protein structures. *J. Appl. Crystallog.* **26**, 283-291.
- Ramakrishnan, C. & Ramachandran, G. N. (1965). Stereochemical criteria for polypeptide and protein chain conformations II. Allowed conformations for a pair of peptide units. *Biophys. J.* **5**, 909-933.
- Luzatti, V. (1952). Statistical treatment of errors in the determination of crystal structures. *Acta Crystallog. sect. A*, **5**, 802-810.
- Herzberg, O., Reddy, P., Reizer, J. & Kapadia, G. (1992). Structure of the histidine-containing phosphocarrier protein HPr from *Bacillus subtilis* at 2.0 Å resolution. *Proc. Natl Acad. Sci. USA*, **89**, 2499-2503.
- Liao, D.-I. & Herzberg, O. (1994). Refined structures of the active Ser83 → Cys and impaired Ser46 → Asp histidine-containing phosphocarrier proteins. *Structure*, **2**, 203-216.
- Jia, Z., Vandonselaar, M., Quail, J. W. & Delbaere, L. T. J. (1993). Active-site torsion angle strain revealed in 1.6 Å-resolution structure of histidine-

- containing phosphocarrier protein. *Nature*, **361**, 94-97.
25. Deutscher, J., Pevce, B., Beyreuther, K., Kiltz, H.-H. & Hengstenberg, W. (1986). *Streptococcal phosphoenolpyruvate* phosphotransferase system: amino acid sequence and site of ATP-dependent phosphorylation of HPr. *Biochemistry*, **25**, 6543-6551.
 26. Thaller, C., Weaver, L. H., Eichele, G., Wilson, E., Karlsson, R. & Jansonius, J. N. (1981). Repeated seeding technique for growing large single crystals of proteins. *J. Mol. Biol.* **147**, 165-469.
 27. Matthews, B. W. (1968). Solvent content of protein crystals. *J. Mol. Biol.* **33**, 491-497.
 28. Sakabe, N. (1983). A focusing Weissenberg camera with multi-layer-line screens for macromolecular crystallography. *J. Appl. Crystallog.* **16**, 542-547.
 29. Otwinowski, Z. & Minor, W. (1997). Processing of X-ray diffraction data collected in oscillation mode. *Methods Enzymol.* **276**, 307-326.
 30. CCP4, (1994). The SERC (UK) Collaborative Computing Project No. 4: a suite of programs for protein crystallography. *Acta Crystallog. sect. D*, **50**, 760-763.
 31. Navaza, J. (1994). AMoRe: an automated package for molecular replacement. *Acta Crystallog. sect. A*, **50**, 157-163.
 32. Roussel, A. & Cambillau, C. (1992). *TURBO-FRODO*, Biographics, Marseilles, France.
 33. Kleywegt, G. J. & Jones, T. A. (1998). Databases in protein crystallography. *Acta Crystallog. sect. D*, **54**, 1119-1131.
 34. Read, R. J. (1986). Improved Fourier coefficients for maps using phases from partial structures with errors. *Acta Crystallog. sect. A*, **42**, 140-149.
 35. Read, R. J. (1990). Structure factor probabilities for related structures. *Acta Crystallog. sect. A*, **46**, 900-912.
 36. Brünger, A. T., Kuriyan, J. & Karplus, M. (1987). Crystallographic *R* factor refinement by molecular dynamics. *Science*, **235**, 458-460.
 37. Brünger, A. T. (1993). *X-PLOR version 3.1*. A system for X-ray crystallography and NMR, Yale University Press, New Haven and London.
 38. Brünger, A. T. (1992). Free *R* value: a novel statistical quantity for assessing the accuracy of crystal structures. *Nature*, **355**, 472-475.
 39. Engh, R. A. & Huber, R. (1991). Accurate bond and angle parameters for X-ray protein-structure refinement. *Acta Crystallog. sect. A*, **47**, 392-400.
 40. Dossionnet, V., Monedero, V., Zagorec, M., Galinier, A., Perez-Martinez, G. & Deutscher, J. (2000). Phosphorylation of HPr by the bifunctional HPr kinase/phosphatase from *Lactobacillus casei* controls catabolite repression and inducer exclusion, but not inducer expulsion. *J. Bacteriol.* **182**, 2582-2590.
 41. Viana, R., Monedero, V., Dossionnet, V., Vadeboncoeur, C., Perez-Martinez, G. & Deutscher, J. (2000). Enzyme I and HPr from *Lactobacillus casei*: their role in sugar transport, carbon catabolite repression and inducer exclusion. *Mol. Microbiol.* **36**, 570-584.
 42. Evans, S. V. (1993). SETOR; hardware-lighted three-dimensional solid model representations of macromolecules. *J. Mol. Graph.* **11**, 134-138.

Edited by P. Wright

(Received 3 August 2000; received in revised form 15 September 2000; accepted 15 September 2000)